PROCEEDINGS OF SCIENCE

Neutron-deuteron scattering (chiral potentials & regulator dependence)

R.Skibiński[*†]
M.Smoluchowski Institute of Physics, Jagiellonian University, PL30-348 Kraków, Poland
E-mail: roman.skibinski@uj.edu.pl

J.Golak
M.Smoluchowski Institute of Physics, Jagiellonian University, PL30-348 Kraków, Poland
E-mail: jacek.golak@uj.edu.pl

V.Soloviov
M.Smoluchowski Institute of Physics, Jagiellonian University, PL30-348 Kraków, Poland
E-mail: volodymyr.soloviov@doctoral.uj.edu.pl

K.Topolnicki
M.Smoluchowski Institute of Physics, Jagiellonian University, PL30-348 Kraków, Poland
E-mail: kacper.topolnicki@uj.edu.pl

V.Urbanevych
M.Smoluchowski Institute of Physics, Jagiellonian University, PL30-348 Kraków, Poland
E-mail: vitalii.urbanevych@doctoral.uj.edu.pl

Yu.Volkotrub
M.Smoluchowski Institute of Physics, Jagiellonian University, PL30-348 Kraków, Poland
E-mail: yuriy.volkotrub@doctoral.uj.edu.pl

H.Witała
M.Smoluchowski Institute of Physics, Jagiellonian University, PL30-348 Kraków, Poland
E-mail: henryk.witala@uj.edu.pl

The predictions for the differential cross section and the deuteron tensor analyzing power T_{22} in nucleon-deuteron elastic scattering based on two chiral models of the nucleon-nucleon interaction are presented and compared with each other and with the data. The recent models at the fifth order of the chiral expansion from the Moscow(Idaho)-Salamanca group and from the Bochum group are used. At the energy of the incoming nucleon E=65 MeV both potentials yield similar data descriptions, however the differences between both models become more significant at E=200 MeV. At the latter energy the dependence of predictions on the used value of the regularization parameter becomes important. In particular, this cutoff dependence is much smaller in the case of the semilocally momentum space regularized potential from the Bochum group.

The 9th International workshop on Chiral Dynamics
17-21 September 2018
Durham, NC, USA

[*]Speaker.

[†]This work is a part of the LENPIC project and is supported by the Polish National Science Centre under Grants No. 2016/22/M/ST2/00173 and No. 2016/21/D/ST2/01120. Numerical calculations were performed on the supercomputer cluster of the JSC, Jülich, Germany.

PoS(CD2018)109

1. Introduction

Various attempts to model nuclear forces were undertaken in the past. The purely phenomenological and semiphenomenological models were used at the beginning of these investigations but these models, which dominated the last few decades of the 20th century, were based on single or multiple boson exchanges. They managed to describe nuclear data with high precision, yielding χ^2/data'99 $\approx$ 1.35 and 1.01 in the case of the two most advanced models, i.e. AV18 [1] and CD Bonn [2], respectively. Nevertheless, the new approaches, which could deliver even more insight into the underlying physics, were sought. Most efforts were focused on models based on the Chiral Effective Field Theory (χEFT) as they ensure a connection to Quantum Chromodynamics and its symmetries and in addition allow a derivation of nuclear two- and many-body forces in a consistent way. At medium energies, where the nucleonic and pionic degrees of freedom are taken into account, two groups have dominated studies of the nucleon-nucleon (NN) interaction: the Bochum-Bonn group and the Moscow(Idaho)-Salamanca collaboration. Both groups have constructed their versions of the NN force and recent models were published in 2018 and 2017, respectively.

The model presented by E.Entem, R.Machleidt and Y.Nosyk in Ref. [3] combines contributions to the nuclear force from the fifth order of the chiral expansion (N^{4}LO) and even supplements them by the sixth order contact F-wave contributions. The resulting potential is relatively soft, nonlocal and a nonlocal regulator is used in the regularization procedure. More details on this force can be found in Refs. [3] and [4]. In particular, in Ref. [3] the authors discuss χ^2/data values depending on the regularization parameter Λ, the order of chiral expansion, the energy range and the isospin channel. As an example we mention that at N^{4}LO and $\Lambda = 500$ MeV, the neutron-proton data up to 290 MeV are described with χ^2/data=1.10.

The newest χEFT based model of the NN interaction was worked out by P.Reinert, E.Epelbaum and H.Krebs and published in Ref. [5]. This model is a successor of the model presented in [6, 7], where for the first time the semilocal regularization was applied. While in [6, 7] the regularization was performed in coordinate space, in the model of Ref.[5] the semilocal regularization was realized in momentum space. This explains the "SMS" term in the name of the model of Ref. [5], which stands for the semilocal momentum-space (regularized potential). However, beside the regularization also other improvements have been introduced in the SMS potential. The most important ones are: fixing the pion-nucleon low energy constants using the Roy-Steiner analysis [8], removing redundant structures in the higher orders of the chiral expansion, and using the Granada self-consistent data base [9] to fix free parameters of the potential. Note that in Ref. [5] the N^{4}LO and N^{4}LO+ (i.e. N^{4}LO plus additional terms from N^{5}LO) forces are discussed separately, but due to the above-mentioned inclusion of the N^{5}LO F-wave contact terms the N^{4}LO potential of Ref. [3] corresponds rather to the N^{4}LO+ force of Ref. [5] than to the pure N^{4}LO interaction from the Bochum group. For further features of the SMS model and a detailed presentation of χ^2/data values we refer the reader to Ref. [5]. To give a comparison with the Moscow(Idaho)-Salamanca force we flash only one example of $\Lambda = 450$ MeV N^{4}LO+ neutron-proton force which describe data up to 300 MeV with χ^2/data=1.06.

While both models, [3] and [5], start from the same Lagrangian, various additional assumptions and technical steps taken to obtain the final form of the potential make the descriptions of the NN data for these models different. It seems that especially the nonequivalent ways of regulariza-

tion give an important contribution to the final difference. In this paper we compare predictions for the nucleon-deuteron (Nd) elastic scattering process for the both models discussed here. We restrict ourselves to two energies of the incoming nucleon: 65 MeV and 200 MeV and neglect the three-nucleon force as well as the Coulomb interaction in the Hamiltonian. While a full analysis of the data description is possible only after including the consistent three-nucleon force, a comparison based on two-body interaction only is a first step in this direction. Note also that up to now no three-nucleon interaction consistent to the Moscow(Idaho)-Salamanca model [3] has been derived and we are not aware of any ongoing or planned work in this direction. In contrast, the derivation of the three-nucleon potential consistent with the SMS NN interaction is much more advanced within the LENPIC collaboration.

Nd scattering is an important tool to study properties of the NN potential as it is a simplest reaction in which the off-shell properties of interaction influence observables. A comprehensive discussion of both Nd elastic scattering and the deuteron breakup predictions based on various semiphenomenological NN models is given in [10]. We also refer the reader to the more recent papers [11, 12, 13, 14] showing, among other things, the application of the chiral interaction with the coordinate space semilocal regularization [6, 7] to the Nd scattering. From these and similar studies it is clear, that a description of 3N observables is a challenging test for models of two- and three-nucleon forces.

The next section gives a short description of our way to obtain the Nd observables, and in Section 3 we present our results on the cross section and the deuteron tensor analyzing power T_{22}.

2. Formalism

To obtain predictions for the Nd elastic scattering observables we use the Faddeev formalism presented in [15], applied to 3N continuum with realistic NN potentials in [16] for the first time, and discussed in detail in [10] and [17].

The NN potential enters this formalism through the t-operator generated via the Lippmann-Schwinger equation. The transition operator for elastic nucleon-deuteron scattering, U, is given as [18]

$$U\Phi = PG_0^{-1}\Phi + PT\Phi + V^{(1)}(1+P)\Phi + V^{(1)}(1+P)G_0T\Phi\,, \tag{2.1}$$

where the auxiliary state $T\Phi$ fulfills the three-nucleon Faddeev equation

$$T\Phi = tP\Phi + (1+tG_0)V^{(1)}(1+P)\Phi + tPG_0T\Phi + (1+tG_0)V^{(1)}(1+P)G_0T\Phi\,, \tag{2.2}$$

with Φ being the initial state composed of the deuteron wave function and a momentum eigenstate of the projectile nucleon. Further G_0 is the free 3N propagator, $P \equiv P_{12}P_{23} + P_{13}P_{23}$ is the permutation operator given in terms of the transpositions P_{ij}, which interchange particles i and j, and $V^{(1)}$ is a part of three-nucleon force symmetrical under the exchange of nucleons 2 and 3.

Neglecting the three-nucleon force Eqs. 2.1 and 2.2 simplify to

$$U\Phi = PG_0^{-1}\Phi + PT\Phi \tag{2.3}$$

and

$$T\Phi = tP\Phi + tPG_0T\Phi\,, \tag{2.4}$$

which we solve in the present studies. We do this in the momentum space using 3N partial-wave states $\mid p,q,\alpha\rangle$ in the jJ-coupling [10, 17, 18]

$$\mid p,q,\alpha\rangle \equiv \mid pq(ls)j(\lambda\frac{1}{2})I(jI)JM_J\rangle \mid (t\frac{1}{2})TM_T\rangle \ , \tag{2.5}$$

where p and q are magnitudes of the Jacobi momenta and α denotes a set of discrete quantum numbers built in the following way: the spin s of the subsystem composed from nucleons 2 and 3 is coupled with their orbital angular momentum l to the subsystem total angular momentum j. The spin $\frac{1}{2}$ of the spectator particle 1 couples with its relative orbital angular momentum λ to the total angular momentum of nucleon 1, I. Finally, j and I are coupled to the total 3N angular momentum J with the projection M_J. For the isospin part, the total isospin t of the (23) subsystem is coupled with the isospin $\frac{1}{2}$ of the spectator nucleon to the total 3N isospin T with the projection M_T.

In the practical realization we take into account all two-body channels up to the two-nucleon total angular momentum $j_{max} = 5$ and the three-nucleon total angular momentum $J_{max} = \frac{25}{2}$. Such a number of partial waves is sufficient to achieve convergence of predictions at the energies for which results are presented here. To be more quantitative, we estimate the uncertainty of the predictions due to the restrictions to the mentioned above partial waves to remain below 0.5%, depending on observables and energy. Some discussion of the convergence can be found in [10] and more recently in [19] where for the deuteron breakup process predictions based on the partial wave decomposition scheme are compared to results obtained without partial wave decomposition, however only in the first-order approximation to the scattering amplitude.

3. Results

In Figs. 1 and 2 we compare predictions for the differential cross sections and the deuteron tensor analyzing power T_{22} at two laboratory energies of the incoming nucleon: E=65 MeV (Fig. 1) and E=200 MeV (Fig. 2). Beside the data we show predictions obtained with the two studied here interactions at N^{4}LO / N^{4}LO+. In both cases we use the value of the regulator parameter $\Lambda = 500$ MeV, however we remind the reader that different methods of regularization are used in these two models.

At E=65 MeV practically no difference between predictions based on the two models is seen for both observables. The observed discrepancies with the cross section data are well understood as a result of neglecting the three-nucleon interaction and the Coulomb force in our calculations. Similar discrepancies are also observed in the case of the semiphenomenological potentials. Also for the T_{22} the chiral predictions resemble the results obtained previously with the other potentials. However, for this observable the nature of the discrepancy around $\theta \approx 145^\circ$ is still unclear. At E=200 MeV a difference between predictions is visible already for the cross section. The SMS model is closer to the data at the minimum of the cross section, so it leaves less room for the three-nucleon force action. In turn, at backward scattering angles the Moscow(Idaho)-Salamanca model is closer to the data. For T_{22} both models give similar predictions but are not able to describe the data, which points to possible three-nucleon force effects. Despite the observed discrepancies and considering the absence of the three-nucleon force both models give a reasonable data description.

In Figs. 3-6 we show the dependence of predictions on the used value of the regulator for the same potentials, energies and observables as discussed above. Fig. 3 and 4 shows predictions at

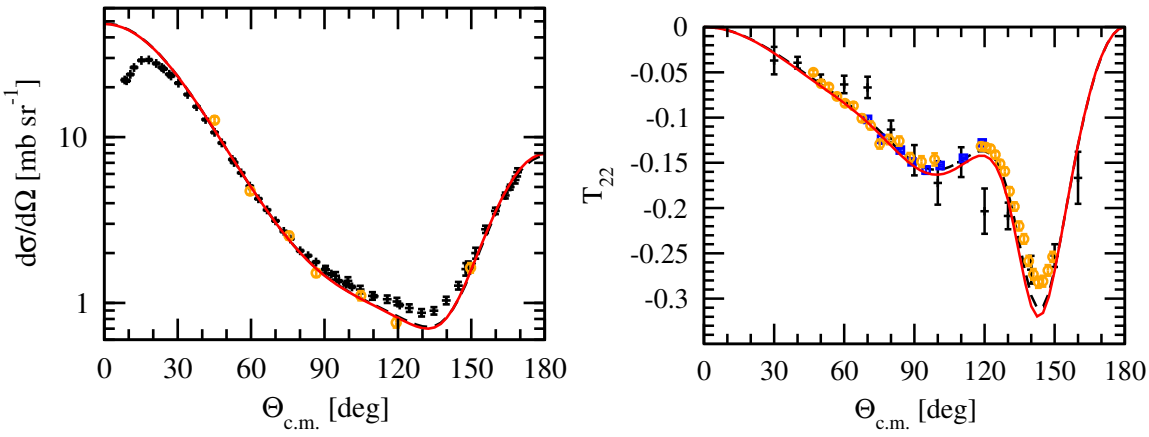

Figure 1: The differential cross section for elastic nucleon-deuteron scattering (left) and the deuteron tensor analyzing power T_{22} (right) at the laboratory nucleon energy E=65 MeV. The dashed black curve represents predictions of the N^{4}LO+ SMS model from the Bochum group with $\Lambda = 500$ MeV and the red line shows predictions of the N^{4}LO Moscow(Idaho)-Salamanca potential with the same value of the Λ regulator. The experimental data for the cross section are from: [20] (*pd* black pluses) and [21] (*nd* orange circles). The data for the T_{22} are from [22] (*pd* black pluses), [23] (*pd* orange circles) and [24] (*pd* blue squares).

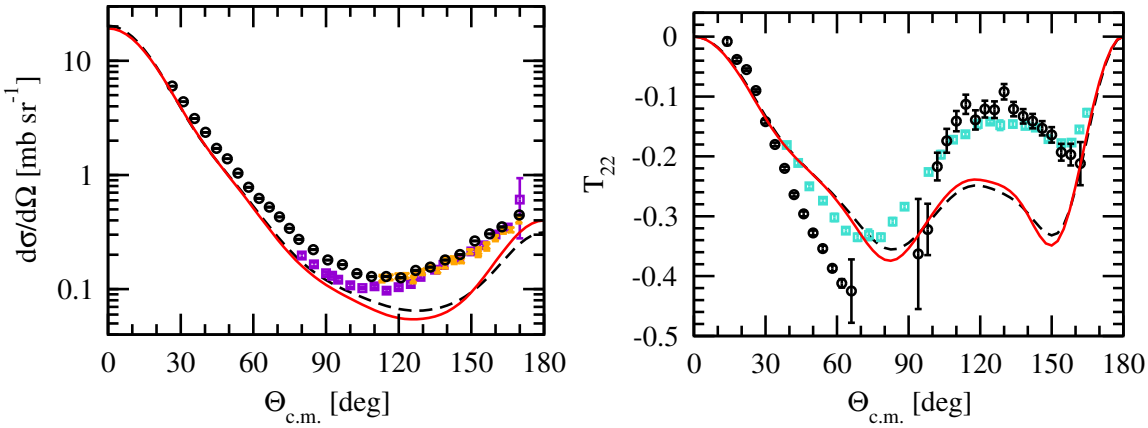

Figure 2: The same as in Fig. 1 but at E=200 MeV. Curves are the same as in Fig. 1. The experimental data for the cross section are from: Ref. [25] (*pd*, $E = 198$ MeV, violet squares), Ref. [26] (*pd*, $E = 180$ MeV, orange x's), and Ref. [27] (*pd*, $E = 198$ MeV, black circles). T_{22} data are from Ref. [28] (*pd* $E = 186.6$ MeV turquoise squares) and Ref. [29] (*pd* $E = 200$ MeV black circles).

E=65 MeV for the SMS model and the Moscow(Idaho)-Salamanca potential, respectively. Following the suggestions of the authors of these interactions we take the following values of the regulators: $\Lambda \in \{400, 450, 500, 550\}$ MeV for the SMS model and $\Lambda \in \{450, 500, 550\}$ MeV in the second case.

At E=65 MeV for the SMS potential practically no cutoff dependence is observed. The predictions based on the Moscow(Idaho)-Salamanca force show only slight cutoff dependence in the case of T_{22}, where the curve representing predictions obtained with $\Lambda = 450$ MeV is slightly separated from the others. But still, the spread of the predictions remains no bigger than the experimental uncertainties. At E=200 MeV the SMS potential continues to work very well for the cross section,

but some cutoff dependence appears for the deuteron tensor analyzing power. The picture is much less in favour of the Moscow(Idaho)-Salamanca model. Fig. 6 shows clearly that various values of the regulator strongly influence the predictions obtained with this potential both for the cross section as well as for T_{22}.

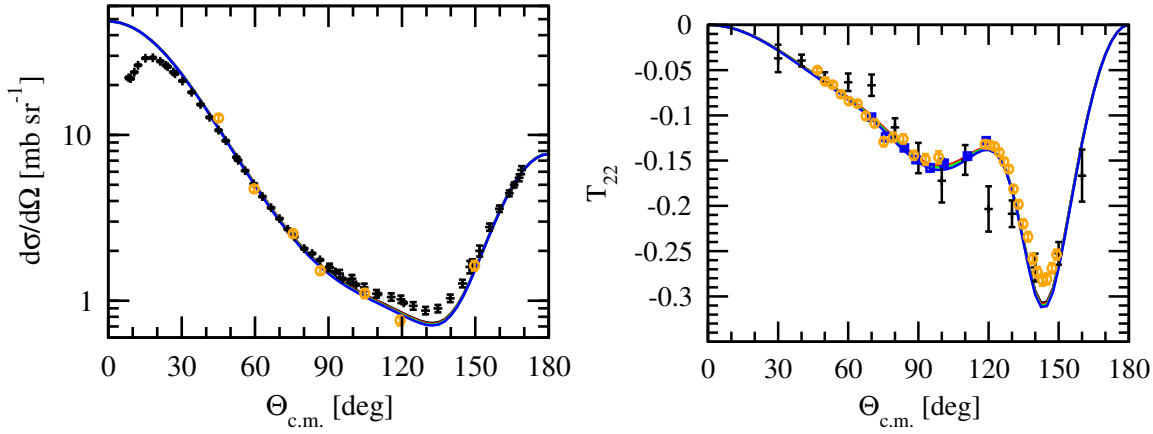

Figure 3: The differential cross section for elastic nucleon-deuteron scattering (left) and the deuteron tensor analyzing power T_{22} (right) at the nucleon laboratory energy E=65 MeV. The predictions have been obtained with the N^{4}LO+ SMS potential. Curves represent predictions obtained with the following values of the regulator parameter Λ: 400 MeV (black), 450 MeV (red), 500 MeV (green), and 550 MeV (blue). The experimental data are the same as in Fig. 1.

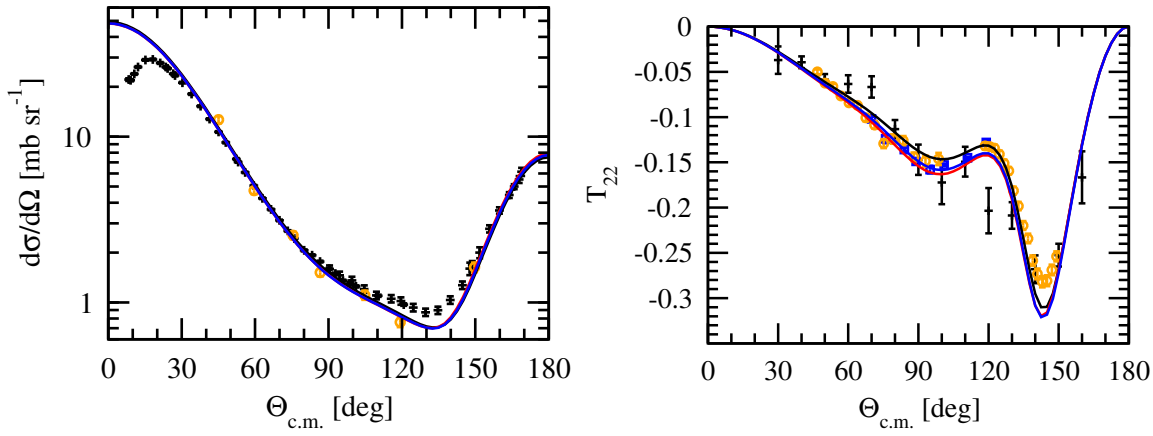

Figure 4: The differential cross section for elastic nucleon-deuteron scattering (left) and the deuteron tensor analyzing power T_{22} (right) at the laboratory nucleon energy E=65 MeV. The predictions have been obtained with the Moscow(Idaho)-Salamanca N4LO potential of Ref. [3]. Curves represent predictions obtained with the following values of the regulator parameter Λ: 450 MeV (black), 500 MeV (red), and 550 MeV (blue). The experimental data are the same as in Fig. 1.

In conclusion we can state that the Nd elastic scattering data descriptions delivered by the two recently derived chiral NN forces: the N^{4}LO+ SMS model from Bochum group [5] and the N^{4}LO Moscow(Idaho)-Salamanca potential [3] are of similar quality. The comparison to data provides a reasonable picture for these two potentials and agrees also with a description provided

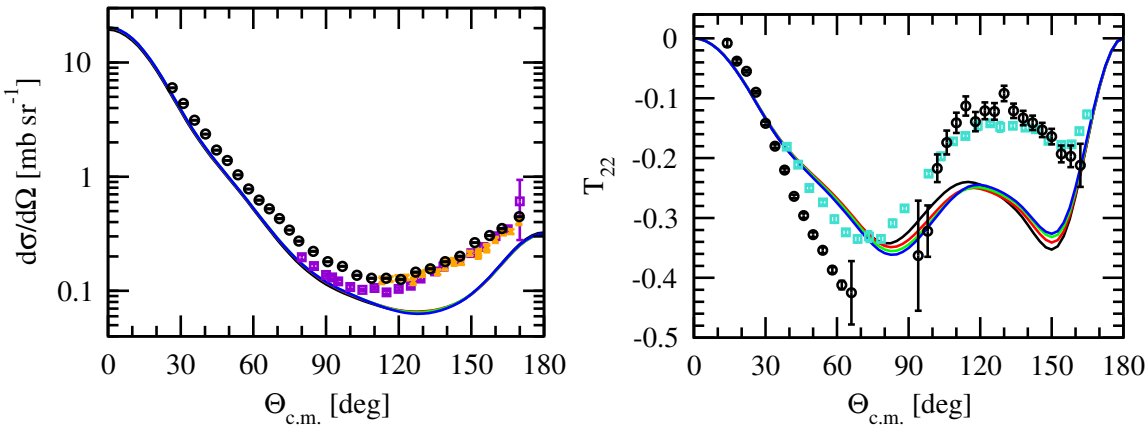

Figure 5: The same as in Fig. 3 but at E=200 MeV. Curves are the same as in Fig. 3. The experimental data are the same as in Fig. 2.

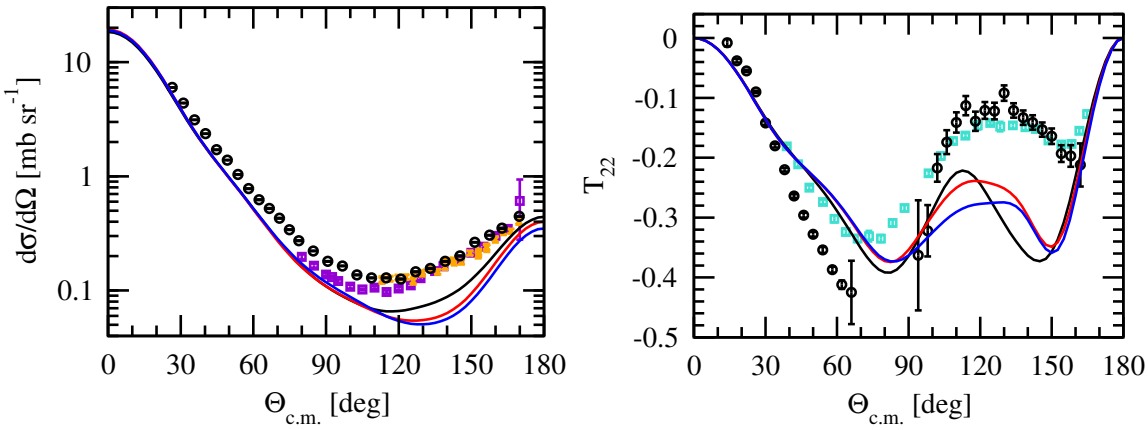

Figure 6: The same as in Fig. 4 but at E=200 MeV. Curves are the same as in Fig. 4. The experimental data are the same as in Fig. 2.

by the semiphenomenological two-nucleon forces. However, the much weaker cutoff dependence observed for the SMS force is a big asset of this model. It remains to check in the future if this property will be present also when the consistent three-nucleon force is taken into account.

References

[1] R. B. Wiringa, V. G. J. Stoks, and R. Schiavilla, Phys. Rev. **C51**, 38 (1995).

[2] R. Machleidt, Phys.Rev. **C63**, 024001 (2001).

[3] D.R. Entem, R. Machleidt, Y. Nosyk, Phys. Rev. **C96**, 024004 (2017).

[4] R. Machleidt, J. Phys.: Conf. Ser. **966**, 012011 (2018).

[5] P. Reinert, H. Krebs, E. Epelbaum, Eur. Phys. J. **A54**, 86 (2018).

[6] E. Epelbaum, H. Krebs, U.-G. Meißner, Phys. Rev. Lett. **115**, 122301 (2015).

[7] E. Epelbaum, H. Krebs, U.-G. Meißner, Eur. Phys. J. **A51**, 53 (2015).

[8] M. Hoferichter, J. Ruiz de Elvira, B. Kubis and U.-G. Meißner, Phys. Rev. Lett. **115**, 192301 (2015).

[9] R. Navarro Pérez, J. E. Amaro, and E. Ruiz Arriola, Phys. Rev. **C88**, 064002 (2013).

[10] W. Glöckle, H. Witała, D. Hüber, H. Kamada and J. Golak, Phys. Rep. **274**, 107 (1996).

[11] S. Binder et al., Phys. Rev. **C93**, 044002 (2016).

[12] S. Binder et al., Phys. Rev. **C98**, 014002 (2018).

[13] E. Epelbaum et al., Phys. Rev. **C99**, 024313 (2019).

[14] H. Witała et al., Few-Body Syst. **60**, 19 (2019).

[15] L.D. Faddeev, Sov. Phys. JETP **12**, 1014 (1961).

[16] H. Witała, Th. Cornelius, W. Glöckle, Few-Body Syst. **3**, 123 (1988).

[17] W. Glöckle, *The Quantum-Mechanical Few-Body Problem* Springer-Verlag, Berlin, 1983.

[18] D. Hüber, H. Kamada, H. Witała and W. Glöckle, Acta Phys. Polon. **B28**, 1677 (1997).

[19] K.Topolnicki et al., Eur. Phys. J. **A51**, 132 (2015).

[20] S. Shimizu et al., Phys. Rev. **C52**, 1193 (1995).

[21] H. Rühl et al., Nucl. Phys. **A524**, 377 (1991).

[22] H. Witała, *et al.*, Few-Body Syst. **15**, 67 (1993).

[23] E. Stephan, *et al.*, Phys. Rev. C **76**, 057001 (2007).

[24] H. Mardanpour, *et al.*, Eur. Phys. J. **A31**, 383 (2007).

[25] R. E. Adelberg, C. N. Brown, Phys. Rev. D **5**, 2139 (1972).

[26] G. Igo *et al.*, Nucl. Phys. A **195**, 33 (1972).

[27] K. Ermisch *et al.*, Phys. Rev. C **71**, 064004 (2005).

[28] K. Sekiguchi *et al.*, Phys. Rev. C **96**, 064001 (2017).

[29] B. von Przewoski *et al.*, Phys. Rev. C **74**, 064003 (2006).